AGU PUBLICATIONS

Global Biogeochemical Cycles

RESEARCH ARTICLE
10.1002/2013GB004773

Key Points:
- NPQ experiments were conducted in the South Atlantic and Southern Ocean
- Significant geographic variability in NPQ characteristics were found
- NPQ correcting satellite fluorescence revealed correlations with iron stress

Supporting Information:
- Readme
- Figure S1
- Figure S2
- Figure S3
- Table S1

Correspondence to:
T. J. Browning,
thomasb@earth.ox.ac.uk

Citation:
Browning, T. J., H. A. Bouman, and C. M. Moore (2014), Satellite-detected fluorescence: Decoupling nonphotochemical quenching from iron stress signals in the South Atlantic and Southern Ocean, *Global Biogeochem. Cycles*, *28*, 510–524, doi:10.1002/2013GB004773.

Received 20 NOV 2013
Accepted 2 MAY 2014
Accepted article online 6 MAY 2014
Published online 20 MAY 2014

Satellite-detected fluorescence: Decoupling nonphotochemical quenching from iron stress signals in the South Atlantic and Southern Ocean

T. J. Browning[1], H. A. Bouman[1], and C. M. Moore[2]

[1]Department of Earth Sciences, University of Oxford, Oxford, UK, [2]Ocean and Earth Science, National Oceanography Centre Southampton, University of Southampton, Southampton, UK

Abstract Satellite-detected sunlight-induced chlorophyll fluorescence could offer valuable information about the physiological status of phytoplankton on a global scale. Realization of this potential is confounded by the considerable uncertainty that exists in deconvolving the multiple ecophysiological processes that can influence the satellite signal. A dominant source of current uncertainty arises from the extent of reductions in chlorophyll fluorescence caused by the high light intensities phytoplankton are typically exposed to when satellite images are captured. In this study, results from over 200 nonphotochemical quenching (NPQ) experiments conducted on cruises spanning from subtropical gyre to Southern Ocean waters have confirmed that satellite fluorescence quantum yields have the potential to reveal broad regions of iron (Fe) stress. However, our results suggest significant variability in phytoplankton NPQ behavior between oceanic regimes. Dynamic NPQ must therefore be considered to achieve a reliable interpretation of satellite fluorescence in terms of Fe stress. Specifically, significantly lower NPQ was found in stratified subtropical gyre-type waters than in well-mixed Southern Ocean waters. Such variability is suggested to result from differences in incident irradiance fluctuation experienced by phytoplankton, with highly variable irradiance conditions likely driving phytoplankton to acclimate or adapt toward a higher dynamic NPQ capacity. Sea surface temperature empirically demonstrated the strongest correlation with NPQ parameters and is presented as a means of correcting the chlorophyll fluorescence signature for the region studied. With these corrections, a decadal composite of satellite austral summer observations is presented for the Southern Ocean, potentially reflecting spatial variability in the distribution and extent of Fe stress.

1. Introduction

Chlorophyll fluorescence is the emission of red light, which, at least under non-nutrient-stressed conditions, arises almost exclusively from chlorophyll-a pigments in photosystem II (PSII), subsequent to excitation by absorbed photons [*Falkowski and Kiefer*, 1985]. Sunlight-induced chlorophyll fluorescence (SICF) has been studied and interpreted as an indicator of chlorophyll concentrations [e.g., *Hu et al.*, 2005], photosynthetic rates [*Kiefer et al.*, 1989; *Topliss and Platt*, 1986], and the photophysiological status of phytoplankton [*Letelier et al.*, 1997; *Morrison*, 2003; *Schallenberg et al.*, 2008; *Behrenfeld et al.*, 2009; *Morrison and Goodwin*, 2010; *Huot et al.*, 2005, 2013; *Westberry et al.*, 2013]. All three of these applications of SICF require estimation or calculation of the quantum yield of fluorescence (ϕ_F, see Table S1 in the supporting information, for all symbols and abbreviations), the ratio of light fluoresced by chlorophyll-a pigments to total light absorbed by phytoplankton. Recently, studies have suggested that higher values of satellite-derived ϕ_F (ϕ_{sat}) could provide an indication of phytoplankton nutrient stress [*Letelier et al.*, 1997; *Huot et al.*, 2005], particularly under Fe-limiting growth conditions [*Behrenfeld et al.*, 2009].

Fe stress has been shown to increase the chlorophyll-a normalized fluorescence of phytoplankton in laboratory and field studies [*Geider et al.*, 1993a; *Sakshaug and Holm-Hansen*, 1977; *Schrader et al.*, 2011]. The exact physiological mechanisms underlying this response are still debated but are thought to be a combination of Fe stress-induced shifts to a higher ratio of photosystem II (PSII) to largely nonfluorescent but highly Fe rich photosystem I (PSI) [*Strzepek and Harrison*, 2004], together with an overexpression of energetically isolated pigment protein complexes [*Schrader et al.*, 2011; *Ryan-Keogh et al.*, 2012; *Behrenfeld and Milligan*, 2013]. In contrast, increases in ϕ_F as a result of macronutrient stress have only been observed

©2014. American Geophysical Union. All Rights Reserved.

where phytoplankton are starved of a macronutrient, thereby inhibiting the production of functional reaction centers [*Kolber et al.*, 1988; *Geider et al.*, 1993b; *Parkhill et al.*, 2001]. Consequently, across extensive regions of the world's oceans where phytoplankton are potentially under conditions of steady state macronutrient limitation rather than starvation (i.e., nutrient availability sets a limit on the standing stock, but nutrient (re)supply may be rapid due to intense recycling [*Moore et al.*, 2013]), it appears that the majority of PSII is fully functional and has relatively low ϕ_F [e.g. *Moore et al.*, 2008]. Regardless of the underlying physiological cause, the empirical relationship between Fe stress and ϕ_F presents an enticing possibility for the remote observation of Fe-stressed growth conditions using satellite-detected ϕ_F [*Behrenfeld et al.*, 2009]. Unfortunately, such a simple relationship is confounded by the fact that Fe stress is not the only control of ϕ_F inferred from satellite data [*Huot et al.*, 2005, 2013; *Schallenberg et al.*, 2008; *Behrenfeld et al.*, 2009].

Variability in two processes, photochemical quenching (qP) and nonphotochemical quenching (NPQ), is particularly important in determining the chlorophyll fluorescence yield under ambient light conditions [*Falkowski and Kiefer*, 1985]. Absorbed photon energy used in the photosynthetic light reactions competes with fluorescence and is termed qP [*Kiefer and Reynolds*, 1992], while NPQ refers to a suite of nonphotochemistry-related mechanisms that can reduce chlorophyll fluorescence [*Müller et al.*, 2001]. These NPQ mechanisms are a direct result of the need to dissipate excess absorbed photon energy as heat to limit photodamage [*Raven*, 2011]. Antennae quenching, which operates on time scales of seconds-minutes, describes thermal dissipation of absorbed photon energy, mainly due to cycling of the xanthophyll pigments [*Demmig-Adams et al.*, 1990], while longer-lived reaction center quenching can be related to photodamage [*Horton et al.*, 1996; *Behrenfeld et al.*, 2009; *Milligan et al.*, 2012].

Satellite images of ocean color are taken near midday under clear-sky conditions, when ϕ_{sat} values are impacted significantly by NPQ mechanisms. A suitable correction for NPQ is therefore essential if ϕ_{sat} is to be used as an indicator for another physiological signal (e.g., Fe stress) [*Dandonneau and Neveux*, 1997; *Maritorena et al.*, 2000; *Morrison*, 2003; *Schallenberg et al.*, 2008; *Behrenfeld et al.*, 2009]. If all phytoplankton populations showed identical trends of fluorescence quenching with increasing irradiance, it would be easy to remove the effect of NPQ from ϕ_{sat} using the particular value of irradiance at the time of satellite image capture. Unfortunately, this appears not to be the case. NPQ has been shown to depend strongly on the light acclimation state of the phytoplankton population [e.g., *Milligan et al.*, 2012], while other potential controls including the phytoplankton species dominating the fluorescence signal and their photoacclimation state remain to be investigated. If NPQ effects cannot be removed confidently, it is clearly impossible to unambiguously ascribe variability in ϕ_{sat} to other physiological signals such as Fe stress.

Previous studies have highlighted the difficulty in correcting ϕ_{sat} signals for NPQ [*Maritorena et al.*, 2000; *Huot et al.*, 2005; *Schallenberg et al.*, 2008; *Behrenfeld et al.*, 2009]. However, thus far NPQ studies in the field have generally been limited to a relatively small number of observations from discrete geographic regions [*Morrison*, 2003; *Schallenberg et al.*, 2008], which were therefore incapable of revealing any ocean-basin scale variability in NPQ characteristics. Taking this into account, alongside evidence suggesting Fe stress increases ϕ_F of phytoplankton [*Geider et al.*, 1993a; *Sakshaug and Holm-Hansen*, 1977; *Schrader et al.*, 2011], the enticing possibility of being able to map regions of Fe stress on a global scale using ϕ_{sat} warrants efforts aimed at improving our understanding of NPQ. To this end, the NPQ of natural phytoplankton assemblages were investigated by detecting changes in ϕ_F under a range of incident light intensities for 229 samples across the South Atlantic and Southern Ocean. These experiments represent the NPQ response of phytoplankton communities from several distinct oceanic regimes: macronutrient-limited subtropical gyre waters; Fe-limited mesotrophic waters; Fe-limited high-nutrient low-chlorophyll waters; and Fe- and macronutrient-replete productive waters. Alongside every measurement the necessary ancillary data for interpretation of responses were collected, including a suite of high-spatial-resolution Fe-addition incubation experiments providing an assessment of Fe stress status in the regions encountered and the direct influence of Fe resupply on fluorescence characteristics. Our results show that ϕ_{sat} holds significant promise for identifying regions of Fe stress provided the NPQ behavior of the particular region can be characterized and hence corrected for. Highlighting potential limitations, we employ an NPQ correction parameter derived from our field observations and present a decadal composite of ϕ_{sat} for the Southern Ocean.

©2014. American Geophysical Union. All Rights Reserved.

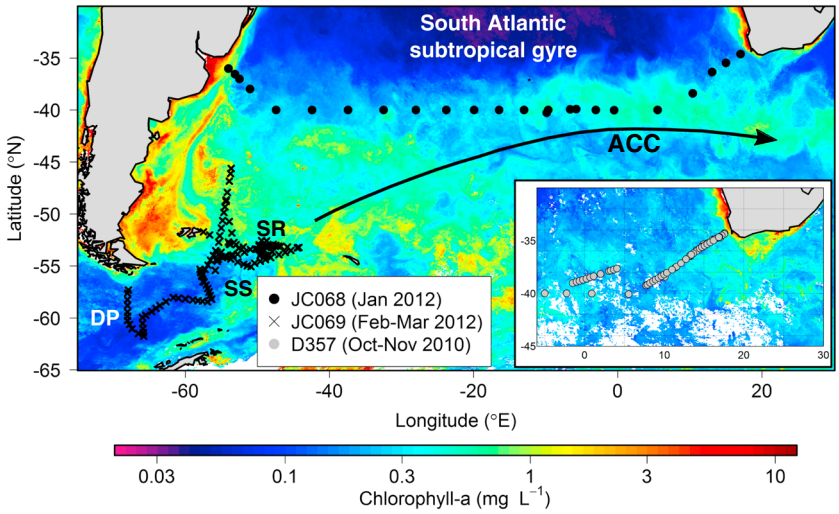

Figure 1. Map of NPQ experiment locations for the different cruises (each symbol represents one experiment). Background is MODIS chlorophyll-a concentration composites for the time periods of the cruises (January–March 2012 for JC068 and JC069; mid-October to mid-November for D357). The general trajectory of the Antarctic Circumpolar Current (ACC) is shown, alongside the locations of Drake Passage (DP), the Scotia Sea (SS), and the Scotia Ridge (SR).

2. Methods

2.1. Cruises

Data were collected on three cruises: two in the South Atlantic (JC068 and D357) and one in the Scotia Sea-Drake Passage region of the Southern Ocean (JC069) (Figure 1). JC068 was carried out during January 2012 and spanned the South Atlantic Basin between 35 and 40°S. D357 occupied the eastern portion of this same transect during October–November 2010. JC069 was undertaken during February–March 2012 and followed a cruise track through the Scotia Sea and Drake Passage.

2.2. Conductivity-Temperature-Depth Data

Vertical profiles of temperature, salinity, fluorescence, and (on occasion for JC068 and D357 cruises) photosynthetically available radiation (PAR) were collected using a Seabird 911 conductivity-temperature-depth and a LI-COR Biospherical PAR sensor. Mixed-layer depths (MLDs) were calculated using the threshold method of *de Boyer Montégut et al.* [2004], while euphotic depth (z_{eu}, assumed to correspond to 1% of surface irradiance) was calculated from PAR profiles for JC068 and D357. For stations without PAR profiles during JC068, a relationship between chlorophyll and the diffuse attenuation coefficient for PAR ($K_{d(PAR)}$) was used to estimate $K_{d(PAR)}$ and therefore z_{eu} using $z_{eu} = 4.6/K_{d(PAR)}$. No underwater PAR data were available for JC069, so $K_{d(PAR)}$ was estimated from

$$K_{d(PAR)} = 0.05 + 0.057\mathrm{Chl}^{0.58}, \quad (1)$$

after *Venables and Moore* [2010] using the Southern Ocean field data of *Korb et al.* [2008] and *Moore et al.* [2007]. A stratification index for the euphotic zone was calculated as the difference in density between a reference surface depth (20 m) and z_{eu}.

2.3. Macronutrient and Trace Metal Concentrations

Dissolved macronutrients silicate, phosphate, and nitrate + nitrite (hereafter referred to as nitrate) were analyzed using a micromolar Bran and Luebbe AAIII segmented flow, colorimetric autoanalyzer using methods described in *Woodward and Rees* [2001]. Samples were analyzed on ship during JC068 and D357 cruises and frozen at −20°C before being analyzed in the UK for JC069.

Surface seawater samples for trace metal analysis and incubation experiments (section 2.8) were collected with a towed fish at 2 to 3 m depth. The seawater was pumped into a trace metal clean sampling container using a Teflon diaphragm pump. Samples were filtered in-line through 0.2 μm cartridge filter (AcroPak1000™) into acid-washed low-density polyethylene sample bottles and acidified with concentrated ultrapure

©2014. American Geophysical Union. All Rights Reserved.

hydrochloric acid (Romil, UpA) to pH 1.6 (0.023 M H^+). Trace metal samples were analyzed using a modified method from *Milne et al.* [2010] by isotope dilution inductively coupled plasma mass spectrometry (Thermo Element XR).

2.4. Phytoplankton Community Structure

High-performance liquid chromatography (HPLC) samples (0.5–2 L) were filtered onto 0.7 μm Whatman GF/F filters, immediately frozen in liquid nitrogen, and then stored in a −80°C freezer. Pigments were extracted into 90% acetone by sonication and analyzed using a Thermo HPLC system following the method described in *Gibb et al.* [2000]. The matrix factorization program CHEMTAX was used to aid with interpretation of the pigments in terms of contributing taxonomic groups to total chlorophyll-a biomass [*Mackey et al.*, 1996]. Starting pigment ratios for the different taxonomic groups were obtained from *Wright et al.* [1996] for Southern Ocean waters and *Veldhuis and Kraay* [2004] for subtropical gyre-type waters. In addition to HPLC analysis, triplicate samples for fluorometric chlorophyll-a analysis (100 mL) were measured on-ship by filtering samples through 0.7 μm Whatman GF/F filter papers, extracting in the dark in 10 mL 90% acetone for 12–24 h in a −20°C freezer, before measuring on a calibrated Turner Designs Trilogy fluorometer [*Holm-Hansen et al.*, 1965].

In addition to pigment analysis, concentrations of nanophytoplankton, photosynthetic picoeukaryotes, *Synechococcus*, and *Prochlorococcus* were analyzed by analytical flow cytometry. Samples (2 mL) were fixed with neutralized paraformaldehyde (1% final concentration) and left for 10 min in the dark at room temperature before being frozen in liquid nitrogen and transferred to a −80°C freezer. Samples were thawed at room temperature and analyzed using a FACSort flow cytometer according to the methods described in *Davey et al.* [2008]. Data analysis and cell counts were carried out in WinMDI Version 2.8 (Joseph Trotter) flow cytometry analysis software.

2.5. Phytoplankton Absorption Spectra

Phytoplankton absorption samples were collected by filtering 0.5–1 L seawater onto 0.7 μm GF/F filters and freezing the filter papers in liquid nitrogen before transferring to a −80°C freezer for storage. Measurements were made using the hot methanol extraction method of *Kishino et al.* [1985] using a Shimadzu UV-2550 spectrophotometer equipped with an integrating sphere over the visible range (350–750 nm). Optical densities for total (i.e., prior to methanol extraction) and detrital (after extraction) particles were corrected for optical path-length amplification arising from scattering by the filter using the method of *Cleveland and Weidemann* [1993]. Phytoplankton absorption coefficients (a_{ph}) were calculated by subtracting the detrital absorption spectra from the total absorption spectra. Pigment-specific absorption coefficients $\left(a^*_{ph}\right)$ were calculated by dividing a_{ph} by HPLC-determined chlorophyll-a concentration. Values of averaged spectrally weighted absorption were calculated by weighting a_{ph} values to (i) a clear-sky irradiance spectrum at the sea surface from measurements in the midlatitude North Atlantic ($<a_{ph}>_{in\ situ}$) and (ii) the spectrum of the blue excitation flashes from the fast repetition rate fluorometer (FRRf) ($<a_{ph}>_{blue}$).

2.6. Fast Repetition Rate Fluorometer and Rapid Light Curves

A FRRf ($FAST^{tracka\ II}$ with integrated $FAST^{act}$ base unit, CTG Ltd.) was used for phytoplankton fluorescence measurements and characterizing NPQ responses. In a single acquisition protocol, the FRRf was set to deliver 64 sequences of one hundred 1 μs subsaturating flashes at 1 μs intervals. Fluorescence transients were fitted to the model of *Kolber et al.* [1998] in FASTpro (V1.5) software (CTG Ltd.). Samples were collected throughout the day-night cycle and were always dark acclimated for at least 30 min prior to analysis (while being maintained at sea surface temperatures). FRRf measurements were corrected for blank fluorescence using 0.2 μm filtrates [*Cullen and Davis*, 2003].

F_v/F_m was calculated as $(F_m - F_o)/F_m$ (where F_o is the fluorescence at t = 0 and F_m is the maximum fluorescence), and functional absorption cross sections (σ_{PSII}) were recovered from the *Kolber et al.* [1998] model fit. A rapid light curve (RLC) protocol was configured to evaluate NPQ for surface samples (JC068, D357, and JC069) and subsurface chlorophyll maximum (SCM) samples (JC068 and D357). The RLC protocol involved a series of identical FRRf single acquisitions (same settings as for single acquisitions, except sequences per acquisition were reduced to 32), performed under a sequence of 14 to 15 progressively increasing PAR ($iPAR_{FRR}$) intensities provided by the $FAST^{act}$ unit, starting from 6 μmol photons $m^{-2}\,s^{-1}$ and

©2014. American Geophysical Union. All Rights Reserved.

increasing to 1434 μmol photons m^{-2} s^{-1}. Each illumination step in the RLCs lasted for 3 min, with 10 s dark steps in between. In order to assess the potential magnitude of spectral differences between the $FAST^{act}$ and solar irradiance, light absorbed by phytoplankton was calculated by weighting $a^*_{ph}(\lambda)$ to the $FAST^{act}$ irradiance spectrum and a clear-sky irradiance spectrum. Differences were relatively minor, with absorption of $iPAR_{FRR}$ being slightly lower (15–25% lower for >90% of samples) and hence to first order could be neglected.

The relative chlorophyll fluorescence quantum yield of dark acclimated samples at F_o and in the light at F' (both of which will be proportional to the actual quantum yields) were calculated as

$$\phi_{rel} = \frac{F_o}{< a_{ph} >_{blue}} \tag{2}$$

and

$$\phi_{rel}{}' = \frac{F'}{< a_{ph} >_{blue}}, \tag{3}$$

respectively. Calculation of relative quantum yield from FRRf data does not require division by $iPAR_{FRR}$, as the contribution of the background irradiance to the fluorescence stimulated during the flash sequence is negligible in comparison with the light-emitting diode flashlets themselves.

Observed relationships between ϕ_{rel}' and irradiance were fitted to the following empirical equation:

$$\phi_{rel}{}' = A \ \ iPAR_{FRR}^{\ B} \tag{4}$$

for $iPAR_{FRR}$ values greater than 300 μmol photons m^{-2} s^{-1}. For values of $iPAR_{FRR}$ lower than 300 μmol photons m^{-2} s^{-1}, the response of ϕ_{rel}' was more complex due to decreasing qP [see, e.g., *Falkowski et al.*, 1986; *Morrison*, 2003]. However, such irradiance levels are not generally representative of those encountered in situ at the time of Moderate Resolution Imaging Spectroradiometer (MODIS) satellite overpasses. We thus initially chose to describe the relationship between ϕ_{rel}' and irradiance using the simple empirical relationship of equation (4), rather than a more mechanistic model [*Morrison*, 2003; *Schallenberg et al.*, 2008; *Morrison and Goodwin*, 2010], both to facilitate more direct comparison with previous basin-scale work [*Behrenfeld et al.*, 2009] and because the presence and quenching characteristics of any potential pool of energetically isolated pigment protein complexes [*Behrenfeld and Milligan*, 2013] would likely complicate the application of currently available mechanistic models [*Morrison and Goodwin*, 2010].

2.7. MODIS Satellite Data Products

Daily, monthly, and seasonal Level 3 MODIS chlorophyll, phytoplankton absorption at 443 nm [*Lee et al.*, 2002], normalized fluorescence line height (nFLH), instantaneous photosynthetically available radiation (iPAR), and sea surface temperature (SST) data products were downloaded for the time periods of the three cruises, in addition to seasonal climatology's for 2002–2012 (http://oceancolor.gsfc.nasa.gov/). All images were from NASA's latest reprocessing (2009 reprocessing for all data pre-2011; 2013 reprocessing for 2011–2013) which includes removal of a temporal trend in nFLH data that existed prior to the 2009 reprocessing (http://oceancolor.gsfc.nasa.gov/REPROCESSING/R2009/modisa_calibration/).

Normalized FLH (nFLH, referred to as F_{sat} in *Behrenfeld et al.* [2009]) is a Level 3 NASA MODIS data product describing fluorescence emanating from the oceans normalized to incident satellite iPAR ($iPAR_{sat}$) [*Abbott and Letelier*, 1999; *Behrenfeld et al.*, 2009]. In order to obtain a quantum yield of fluorescence, values of nFLH need to be corrected for the fraction of $iPAR_{sat}$ actually absorbed by phytoplankton. Following the method of *Behrenfeld et al.* [2009], fields of spectrally averaged phytoplankton absorption were initially estimated from satellite-derived chlorophyll-a concentrations (Chl_{sat}) using the equation of *Bricaud et al.* [1998]:

$$< a_{ph} >_{in\ situ} = Chl_{sat} < a^*_{ph} >_{in\ situ} = A_p Chl_{sat}^{E_p}, \tag{5}$$

where $< a_{ph} >_{in\ situ}$ is the average spectrally weighted phytoplankton absorption coefficient, $< a^*_{ph} >_{in\ situ}$ is the average chlorophyll-specific absorption coefficient, and A_p and E_p are parameters from an empirical data fit (see Figure S1 in the supporting information). A_p and E_p were initially set to 0.0147 and 0.684, respectively, as calculated by *Behrenfeld et al.* [2009] who used the data of *Bricaud et al.* [1998]. Subsequently, values were determined from our own data set (see section 2.5) to investigate the importance of regional variation in

©2014. American Geophysical Union. All Rights Reserved.

these parameters for resultant ϕ_{sat} fields. Satellite fields of a_{ph} at 443 nm [*Lee et al.*, 2002] were also investigated as a means of normalizing the fluorescence signal directly to phytoplankton absorption.

The final ϕ_{sat} algorithm of *Behrenfeld et al.* [2009], including corrections for phytoplankton absorption and other satellite corrections [see *Behrenfeld et al.*, 2009], is as follows:

$$\phi_{sat} = 0.01 \frac{\mathrm{nFLH}}{< a_{ph} >}. \quad (6)$$

As an initial approximation of NPQ, *Behrenfeld et al.* [2009] then applied a 1/iPAR correction in the form

$$\mathrm{NPQ-corrected}\ \ \phi_{sat} = \phi_{sat} \frac{\mathrm{iPAR}}{1590}, \quad (7)$$

where 1590 is equal to MODIS global average iPAR for the time period of their study (units of μmol photons $m^{-2}\,s^{-1}$).

The geometric calculation of nFLH [see *Abbott and Letelier*, 1999] should in theory remove any artifact introduced due to fluorescence from colored dissolved organic matter (as is directly characterized in the field with the blank FRRf measurements described in section 2.6), which is supported by observations of spectrally resolved colored dissolved organic matter (CDOM) fluorescence by *Chekalyuk and Hafez* [2008]. Therefore, despite CDOM fluorescence being found to contribute significantly to total fluorescence in the most oligotrophic waters encountered, as elsewhere [*Moore et al.*, 2008], the baseline method used for the calculation of nFLH should in theory remain robust in these systems. However, we follow the recommendation of *Huot et al.* [2013], who suggest that uncertainty in satellite-detected chlorophyll and fluorescence increases significantly below chlorophyll concentrations of 0.1 mg m^{-3}, in subsequent analysis by highlighting pixels with chlorophyll-a < 0.1 mg m^{-3} and suggesting these be interpreted with caution.

2.8. Fe-Addition Incubation Experiments

Fe-addition incubation experiments were performed using trace metal clean seawater from the towed fish and followed the method described in *Ryan-Keogh et al.* [2013] and *Browning et al.* [2014]. Fe-limited waters were defined as those producing a statistically significant ($p < 0.01$ level using a one-tailed Student's *t* test) F_v/F_m increase in Fe-amended bottles over that of control (non-amended) bottles. Values of $\Delta F_v/F_m$ were calculated, where $\Delta F_v/F_m$ = average F_v/F_m Fe-amended bottles − average F_v/F_m control bottles [*Ryan-Keogh et al.*, 2013].

3. Results and Discussion

3.1. Biogeochemical Regimes Encountered on Cruises

Collectively, the three cruises encountered several oceanic provinces [*Longhurst*, 1998]. JC068 passed through two clear regimes in either side of the south subtropical convergence (SSTC), which is described in detail in *Browning et al.* [2014]. Warmer subtropical gyre-type waters next to the South African coast and in the Western Atlantic Basin were characterized by low macronutrient concentrations, low surface chlorophyll-a concentrations, distinct subsurface chlorophyll maxima (SCMs), and elevated concentrations of smaller cells including *Synechococcus* and *Prochlorococcus*. Conversely, colder sub-Antarctic–Antarctic Circumpolar Current (ACC) waters to the south of the SSTC had elevated macronutrient concentrations, uniform chlorophyll-a concentrations through the mixed layer, and low concentrations of picocyanobacterial cells. ACC waters were shown to be Fe limited on the basis of significant (*t* test $p < 0.01$) increases in F_v/F_m following Fe amendment, while within subtropical gyre-type waters, the standing crop of phytoplankton was likely limited by macronutrient availability [*Browning et al.*, 2014]. D357 was carried out in the eastern portion of the JC068 transect during austral spring when the SSTC was occupying a more northerly location. Consequently, the regime encountered was predominantly that of the ACC waters in the JC068 cruise.

JC069 passed through productive waters close to the South American continental shelf (chlorophyll-a concentrations >2 mg m^{-3}), both high- and low-chlorophyll-a filaments around the Scotia Ridge, and low chlorophyll-a waters in Drake Passage (lowest surface concentration of <0.03 mg m^{-3}). Macronutrient concentrations increased from relatively low values next to the South American shelf (minimum of 1.8 μmol L^{-1} nitrate) to high values in the Scotia Sea and Drake Passage (up to 27.8 μmol L^{-1} nitrate).

©2014. American Geophysical Union. All Rights Reserved.

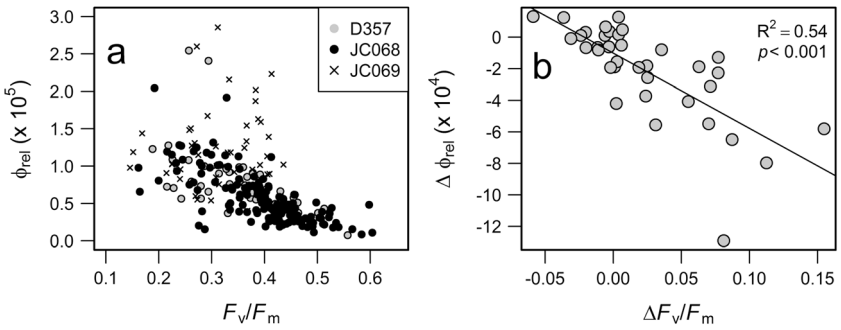

Figure 2. Field-based measurements of ϕ_{rel} and F_v/F_m. (a) Nighttime ϕ_{rel} versus F_v/F_m for the three cruises. (b) Inverse co-variability of phytoplankton response to Fe addition in terms of F_v/F_m and ϕ_{rel} parameters. Delta notation indicates the difference between Fe-amended bottles and control bottles in terms of F_v/F_m and ϕ_{rel} parameters. For Figure 2b, $< a_{ph} >_{blue}$ (i.e., as required in equation (2)) was derived from its relationship with fluorometrically determined chlorophyll-a concentration for each of the two cruises where incubation experiments were performed.

Phytoplankton community structure transitioned from a mixed population co-dominated by haptophytes and diatoms around the Scotia Ridge to haptophyte-dominated waters in the Drake Passage. Physiological responses of phytoplankton to Fe replenishment were observed throughout this cruise but showed no clear spatial trend.

3.2. Correlation of ϕ_{sat} With In Situ Matchups

F_v/F_m has been used routinely as an index of Fe limitation [*Behrenfeld and Milligan*, 2013], with fluorescence quantum yields (or more typically, chlorophyll normalized values of F_o or F_m), being reported less frequently. Overall, ϕ_{rel} and F_v/F_m were observed to be negatively correlated within the current study, although there was some evidence of cruise and/or spatial variability in the observed relationships (Figure 2a). Furthermore, inverse co-variability was observed between the response of ϕ_{rel} and F_v/F_m to Fe replenishment (Figure 2b), confirming that higher values of ϕ_{rel} were likely associated with regions of Fe stress across our wider study area.

Calculation of ϕ_{sat} values with the potential to reliably indicate relative levels of Fe stress requires appropriate NPQ correction and realistic parameterization of light absorption by phytoplankton. Although light absorption by phytoplankton can be estimated on the basis of an empirical relationship with satellite-derived chlorophyll-a concentrations (e.g., equation (5) and Figure S1 in the supporting information), such relationships tend to be characterized by large scatter, and hence, it may be desirable to use satellite products representing phytoplankton absorption directly [*Lee et al.*, 2002; *Westberry et al.*, 2013]. However, while same-day matchups between remote sensing observations and in situ data revealed a good correlation for chlorophyll-a ($R^2 = 0.92$, $p < 0.001$; see Figure S2b in the supporting information), for phytoplankton absorption at 443 nm, the correlation was markedly worse ($R^2 = 0.18$, $p = 0.08$; Figure S2d in the supporting information), and hence, we currently still rely on indirect phytoplankton absorption inferred from chlorophyll-a.

Attempts were made to calculate satellite fields of phytoplankton absorption using a regional relationship between phytoplankton absorption and surface chlorophyll concentration based on in situ observations (Figure S1 in the supporting information); however, a lack of data points at high chlorophyll values resulted in poorly constrained nonlinear model fits that propagated to lower chlorophyll values. This problem has been commented on previously when similar regional data sets have been used [*Stuart et al.*, 2000; *Sathyendranath et al.*, 2001]. To overcome this, we followed the method of *Behrenfeld et al.* [2009] who used the extensive, global absorption-chlorophyll data set of *Bricaud et al.* [1998]. This data set is much better constrained at higher chlorophyll concentrations (up to 25 mg chlorophyll-a m^{-3}). Potential bias may be introduced in using this model generated using data largely collected outside the Southern Ocean. In particular, the low chlorophyll values in the data set of *Bricaud et al.* [1998] are biased to low-latitude, gyre-type waters dominated by picocyanobacteria rather than picoeukaryotes and nanoeukaryotes which dominate the low-chlorophyll waters of the Southern Ocean [*Bouman et al.*, 2012]. Indeed, our data (Figure S1 in the supporting information), along with other data sets from the Southern Ocean [*Mitchell and Holm-Hansen*, 1991;

©2014. American Geophysical Union. All Rights Reserved.

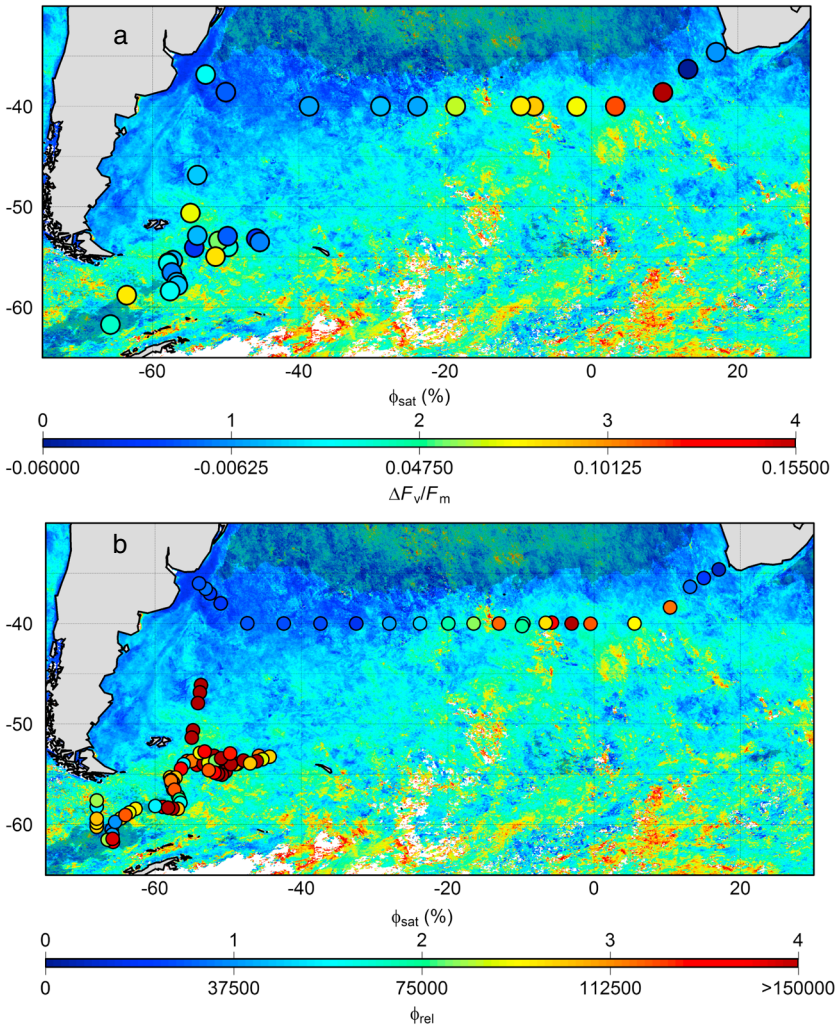

Figure 3. Satellite fluorescence quantum yield and field matchups for the three cruises. (a) January–March 2012 (JC068 and JC069 cruise period) averaged ϕ_{sat} (not NPQ corrected) with $\Delta F_v/F_m$ measurements overplotted. (b) Same as Figure 3a but with ϕ_{rel} overplotted. Pixels with chlorophyll-a less than 0.1 mg m^{-3} in Figures 3a and 3b are shaded.

Reynolds et al., 2001], show absorption values which fall below the best fit line of *Bricaud et al.* [1998] (i.e., lower absorption per chlorophyll-a concentration), likely as a result of a reduced contribution of photoprotective pigments to absorption, alongside increased pigment packaging effects due to generally larger cell sizes in these waters [e.g., *Morel and Bricaud*, 1981; *Reynolds et al.*, 2001].

Correcting ϕ_{sat} for absorption but not NPQ (Figure 3; also see Figures S2 and S3 in the supporting information) revealed broadly similar, oceanographically coherent spatial patterns in ϕ_{sat} and the proximal response of the phytoplankton community to Fe replenishment as indicated by $\Delta F_v/F_m$, as well as ϕ_{sat} and dark acclimated values of ϕ_{rel} (Figures 3a and 3b, respectively). Greater variability observed for both $\Delta F_v/F_m$ and ϕ_{rel} in the Scotia Sea region may result from high spatial dynamics in phytoplankton ecophysiology [*Holm-Hansen et al.*, 2004] driven by the dynamic mixing environment that exists in this region [e.g., *Naveira Garabato et al.*, 2004], which consequently may cause longer time period composites to mask shorter time scale variability as observed in field measurements. Consistent with this, the limited number of same-day satellite matchups tended to show significantly better correlations for a range of retrieved products (see Figure S3 in the supporting information). Although this initial relationship between non-NPQ corrected values of ϕ_{sat} with regions of Fe stress appears promising, we now consider whether significant differences in NPQ between regions could be resulting in biased satellite observations of ϕ_{sat}.

©2014. American Geophysical Union. All Rights Reserved.

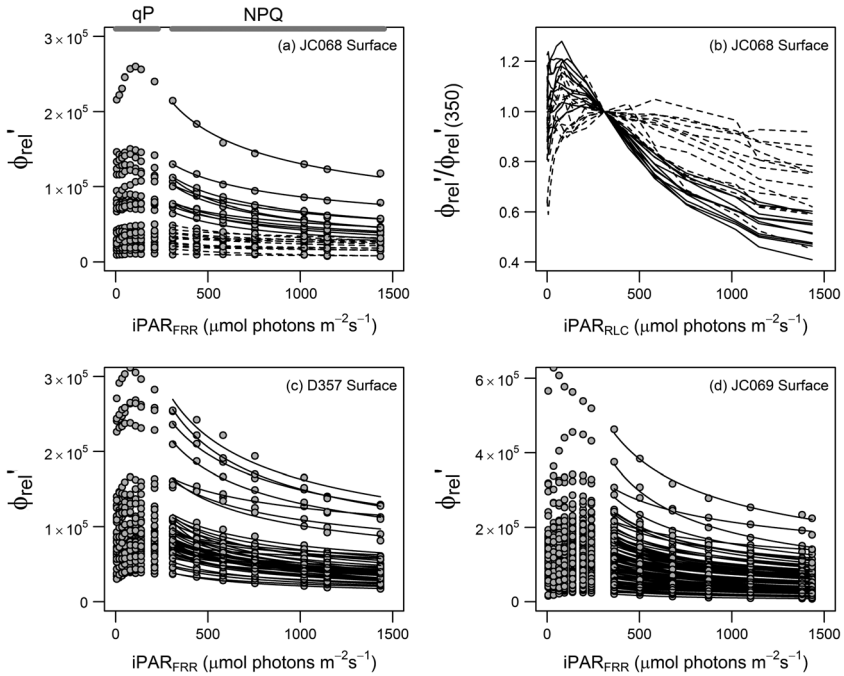

Figure 4. (a–d) ϕ_{rel} response of surface samples for the three cruises. Dots represent data points, and curves in Figures 4a, 4c, and 4d represent best fit models to data points at iPAR > 300 μmol photons $m^{-2}s^{-1}$. Dominant regions of qP and NPQ are highlighted in Figure 4a. Figure 4b shows NPQ for surface waters in the two ecophysiological regimes encountered on JC068: ϕ_{rel}' at each light step have been normalized to ϕ_{rel}' at 350 μmol photons $m^{-2}s^{-1}$ to remove the influence of Fe limitation on yields. Resultant curves with steeper gradients have greater NPQ. Dashed lines in Figures 4a and 4b distinguish the two distinct ecophysiological regimes identified on JC068 (see main text).

3.3. Controls on Nonphotochemical Quenching

Field measurements of ϕ_{rel}' at progressively increasing iPAR showed significant variability in observed NPQ responses, with the relationship between ϕ_{rel}' and $iPAR_{FRR}$ varying for both surface (Figure 4) and SCM samples (not shown) for all cruises. In particular, the curves for JC068 could clearly be divided into two distinct zones of high and low NPQ which also corresponded to the two dominant ecophysiological regimes encountered on the cruise. Specifically, flatter relationships indicating minimal dynamic NPQ were observed in the warmer, low-nitrate, Fe-replete subtropical gyre-type waters (Figure 4a, dashed lines), while enhanced dynamic NPQ was observed in the colder, high-nitrate, Fe-limited (ACC type) waters (Figure 4a, solid lines). Normalizing to low light values further emphasized that NPQ-driven reductions in ϕ_{rel}' from ACC waters sampled on JC068 were typically around double that of the modest response observed in subtropical gyre waters (Figure 4b). Less coherent geographical variability was observed during the D357 and JC069 cruises; however, a considerable spread of NPQ responses remained (Figures 4c and 4d).

In order to provide an index of the NPQ response, we fitted values of ϕ_{rel} at the upper range (>300 μmol photons $m^{-2}s^{-1}$) of $iPAR_{FRR}$ to equation (4), to obtain the empirical parameter *B* [e.g., *Milligan et al.*, 2012]. A wide range of *B* values were found (between −0.84 and −0.057 for all experiments) with strong spatial variability, suggesting that any robust NPQ correction method would have to account for such differences. Consequently, for the regions encountered on our cruises, a single $iPAR^{-1}$ correction, i.e., an assumed value of −1 for *B*, as used as an initial approximation in previous studies [*Behrenfeld et al.*, 2009], would not be capable of accurately accounting for NPQ, with highest discrepancies likely for subtropical gyre-type waters which displayed much lower dynamic NPQ at high iPAR.

In order to investigate potential ecophysiological drivers of the variable NPQ responses, correlation analyses were carried out between *B* and potential controlling factors (Figure 5). Despite almost certainly exerting some degree of control over fluorescence characteristics [e.g., *Suggett et al.*, 2009] and therefore NPQ variability, neither trophic status (i.e., chlorophyll-a concentration) nor community structure (apart from cyanobacteria presence) showed a clear relationship with *B* (Figures 5f–5h). Similarly, varying levels of Fe

©2014. American Geophysical Union. All Rights Reserved.

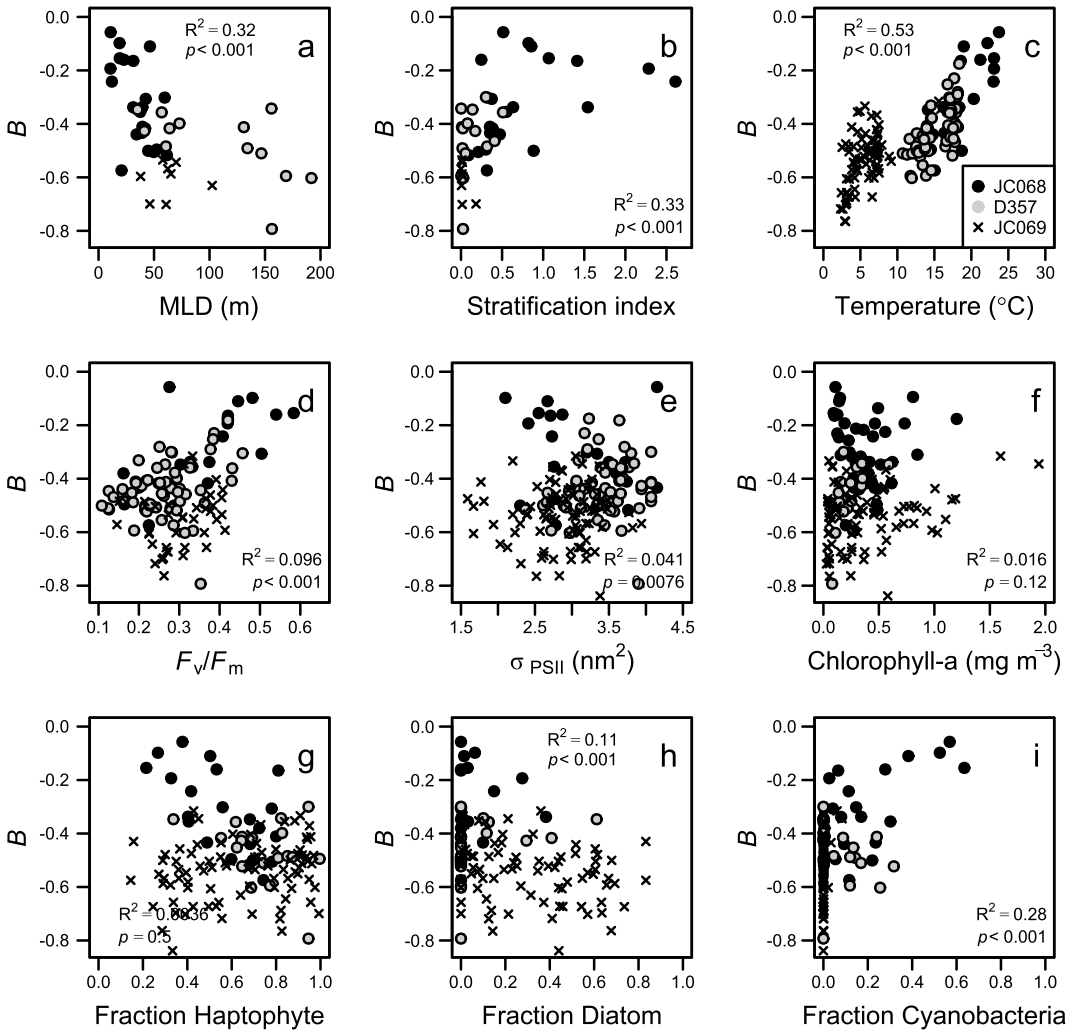

Figure 5. Relationships between *B*, the exponent representing ϕ_{rel}' decay in equation (4), and possible controls (surface samples only).

stress have been suggested to potentially enhance NPQ [*Cullen*, 2009]; however, the correlation of *B* with F_v/F_m was weak ($R^2 = 0.096$, $p < 0.001$), suggesting that this is unlikely the dominant driver (Figure 5d). In contrast, derived values of *B* were more strongly correlated with parameters relating to the light environment phytoplankton were experiencing. Observed relationships between *B* and mixed-layer depths (MLDs) ($R^2 = 0.32$, $p < 0.001$) and stratification indices ($R^2 = 0.33$, $p < 0.001$) both suggested that the highest dynamic NPQ responses occurred under conditions of deeper mixing and/or reduced near-surface stratification (Figures 5a and 5b), as might be expected for phytoplankton populations having to cope with the more variable light regimes encountered in these environments, as compared to highly stratified systems. Such a pattern is consistent with laboratory studies of marine diatoms [*Milligan et al.*, 2012; *Lavaud et al.*, 2007]. Data from the fluorometer linked to the ships' underway flow-through system further supported these observations, with the typically observed diel fluorescence cycles characterized by daytime reductions [e.g., *Dandonneau and Neveux*, 1997] suggestive of much greater NPQ within the regions of deeper mixed layers on JC068 (not shown).

While being an unlikely candidate for driving NPQ variability at the physiological level, a clear correlation of *B* with sea surface temperature (SST) was found ($R^2 = 0.53$, $p < 0.001$) (Figure 5c). Such a relationship further highlights the strong geographical variability in the extent of NPQ. Moreover, SST is suggested to be a good predictor of *B* due to the relationship between upper ocean temperature with the extent of near-surface stratification and MLD [*Bouman et al.*, 2003]. Consequently, relationships between the extent of NPQ (*B*) and

©2014. American Geophysical Union. All Rights Reserved.

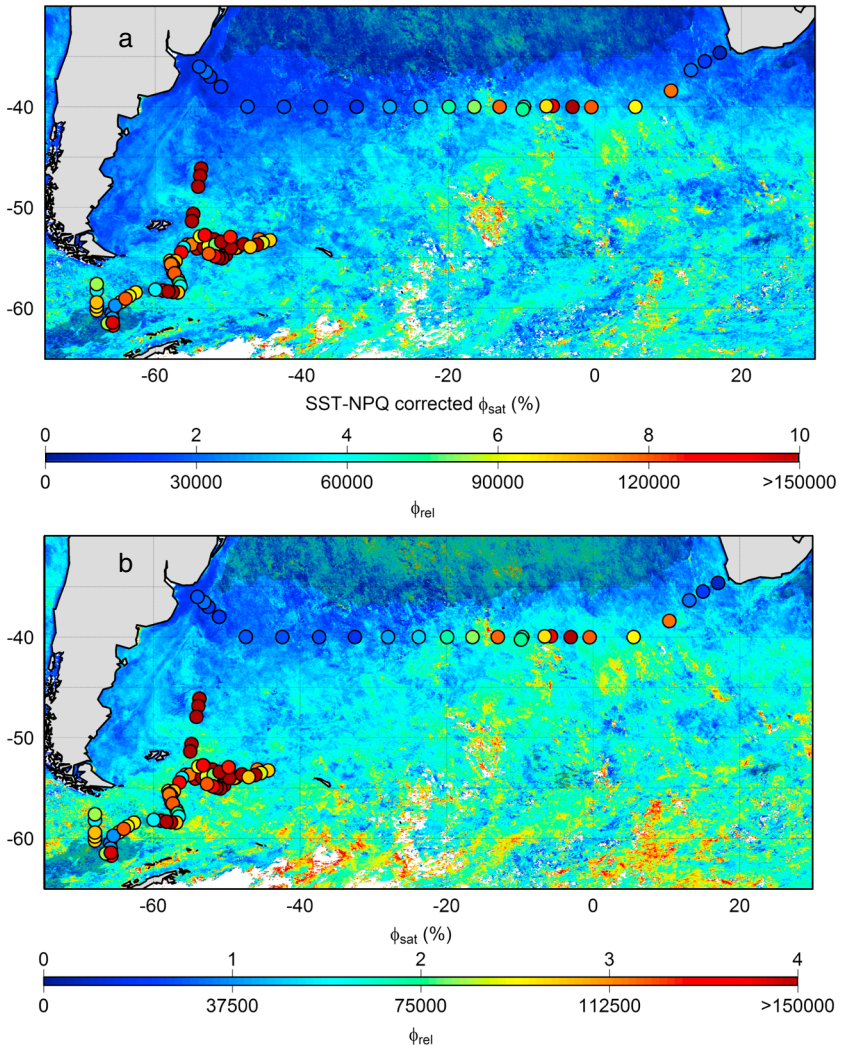

Figure 6. NPQ-corrected ϕ_{sat} for January–March 2012 with field measurements of ϕ_{rel} overplotted. Two NPQ corrections have been applied: (a) 1/iPAR NPQ correction and (b) SST-NPQ correction. Note that for Figure 6b, the correction function was only applied over the SST range for NPQ experiments (2 to 24°C). Pixels with chlorophyll-a less than 0.1 mg m^{-3} are shaded.

community structure (i.e., with cyanobacteria: $R^2 = 0.28$, $p < 0.001$; Figure 5i) may also be noncausal, with both responding instead to the same driver [*Margalef*, 1978; *Cushing*, 1989]. Irrespective of the underlying controls, correlation between the extent of NPQ and SST is clearly of potential utility in NPQ-correcting fields of ϕ_{sat}.

3.4. Correcting for NPQ Using SST

The observed linear model regression between B and SST allowed us to empirically predict values of B using satellite-retrieved values of SST (Figure 5c):

$$B = 0.019\mathrm{SST} - 0.65. \tag{8}$$

Subsequent fields of B were hence used to NPQ-correct ϕ_{sat} to values expected at low light intensities according to

$$\phi_{sat}(\mathrm{SST}) = \phi_{sat}\left(\frac{350}{\mathrm{iPAR}_{sat}}\right)^{B}, \tag{9}$$

where ϕ_{sat} (SST) represents ϕ_{sat} with the SST-derived NPQ correction applied, 350 represents the low-light iPAR value chosen as the normalization point (units of μmol photons m^{-2} s^{-1}), and iPAR_{sat} represents irradiance at the time of image capture (units of μmol photons m^{-2} s^{-1}).

©2014. American Geophysical Union. All Rights Reserved.

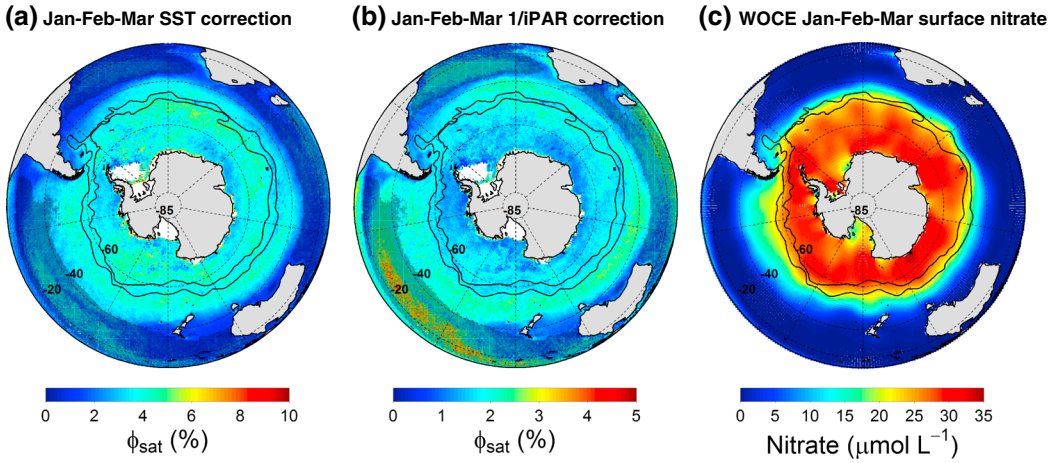

Figure 7. Southern Ocean 2002–2012 austral summertime composites of (a) NPQ (SST)-corrected ϕ_{sat} (note that we have included data beyond the latitudinal bounds of our experiments, and these regions should thus be interpreted with caution); (b) 1/iPAR-corrected ϕ_{sat}; and (c) World Ocean Circulation Experiment (WOCE) austral summertime nitrate concentrations (http://woce.nodc.noaa.gov/wdiu/). Pixels with chlorophyll-a less than 0.1 mg m^{-3} in Figures 7a and 7b are shaded. Black lines show locations of polar (inner) and sub-Antarctic (outer) fronts from *Orsi et al.* [1995].

Using this correction, ϕ_{sat} (SST) fields were derived for the geographic region and time period of our cruises (Figure 6a). As for field measurements of ϕ_{rel}, SST-NPQ-corrected ϕ_{sat} fields indicated strong geographic variability, with ACC waters having elevated ϕ_{sat} relative to both low-chlorophyll (elevated SST) subtropical gyre-type waters and high-chlorophyll (low SST) waters west of Patagonia. For comparison, applying a 1/iPAR correction (equation (7) [*Behrenfeld et al.*, 2009] to the same data (Figure 6b) resulted in clear differences, with higher ϕ_{sat} predicted in stratified subtropical gyres and lower ϕ_{sat} at high latitudes as a result of overprediction and underprediction of the actual extent of NPQ in these regions, respectively.

3.5. Decadal Composite of NPQ-Corrected ϕ_{sat}

Extending the NPQ (SST) correction to all circumpolar waters for a 2002–2012 austral summer composite revealed clear spatial patterns in ϕ_{sat} (Figure 7a). Given the uncertainties involved in calculating ϕ_{sat}, caution clearly still needs to be applied in attributing such spatial variability to Fe stress, although our field observations lend support to such an interpretation. Indeed, elevated values of the climatology of NPQ-corrected ϕ_{sat} (using SST) spatially correlated with summertime elevated nitrate (Figure 7c) and hence the broad so-called high-nitrate low-chlorophyll regime expected to be characterized by Fe stress [*Moore et al.*, 2013]. In contrast, using a 1/iPAR NPQ correction [*Behrenfeld et al.*, 2009], which cannot account for spatial variability in the NPQ relationships we observed, produced fields of ϕ_{sat} which do not correlate with elevated summertime nitrate, in particular decreasing significantly south of 60°S and increasing in the subtropics (Figure 7b). Finer-scale spatial variability in SST-NPQ-corrected ϕ_{sat} might subsequently be related to regional-scale Fe sources, for example, over the Patagonian shelf and other potential sedimentary sources, dust deposition [*Cassar et al.*, 2007], deep water upwelling [*de Baar et al.*, 1995; *Lefèvre and Watson*, 1999], or iceberg discharge [*Raiswell et al.*, 2008].

4. Conclusions and Future Directions

Decades of field work on ships has been required to map regions of Fe stress [*Moore et al.*, 2013] and hence the ability to retrieve such information globally at high temporal frequency using remote sensing observations of chlorophyll fluorescence is an exciting possibility [*Behrenfeld et al.*, 2009]. However, thus far uncertainty in phytoplankton NPQ behavior has limited realization of this potential. Here we have developed and applied a dynamic SST-based NPQ correction for ϕ_{sat} and suggest there is a strong likelihood that the resulting product may be indicative of relative Fe stress levels. However, while our field data do span several biogeochemical provinces, we advise caution when interpreting SST-NPQ-corrected ϕ_{sat} beyond the sampled region. Two factors of particular concern are (i) the applicability of such an NPQ correction in other regions and seasons, and

©2014. American Geophysical Union. All Rights Reserved.

(ii) potential artifacts associated with satellite-retrieved chlorophyll concentrations and fluorescence when chlorophyll is less than 0.1 mg m^{-3} [*Huot et al.*, 2013].

Characterizing NPQ behavior throughout the world's oceans may ultimately allow less biased global maps of ϕ_{sat} to be attained. Although conducting sufficient numbers of dedicated experiments would be a significant task, as suggested above, fluorescence data routinely collected from ships' underway flow-through systems could allow broad characterization of NPQ regimes. Establishment of robust relationships could subsequently facilitate less ambiguous attribution of variability in ϕ_{sat} to Fe stress across broad spatiotemporal scales.

Acknowledgments

We thank the officers, crew, technicians, and scientists for their help on UK-GEOTRACES JC068 and D357, and DIMES JC069, cruises. Christian Utschig is acknowledged for his help in running the phytoplankton absorption spectra. Michael Behrenfeld and an anonymous reviewer are both thanked for comments which significantly improved this paper. This work was funded by the UK-GEOTRACES National Environment Research Council (NERC) Consortium grant (NE/H006095/1) which included a studentship to T.J.B.

References

Abbott, M. R., and R. M. Letelier (1999), Algorithm theoretical basis document chlorophyll fluorescence, MODIS product number 20, NASA. [Available at http://modis.gsfc.nasa.gov/data/atbd/atbdmod22.pdf.]

Behrenfeld, M. J., and A. J. Milligan (2013), Photophysiological expressions of iron stress in phytoplankton, *Annu. Rev. Mar. Sci.*, *5*, 217–246, doi:10.1146/annurev-marine-121211-172356.

Behrenfeld, M. J., et al. (2009), Satellite-detected fluorescence reveals global physiology of ocean phytoplankton, *Biogeosciences*, *6*(5), 779–794, doi:10.5194/bg-6-779-2009.

Bouman, H. A., et al. (2003), Temperature as indicator of optical properties and community structure of marine phytoplankton: Implications for remote sensing, *Mar. Ecol. Prog. Ser.*, *258*, 19–30, doi:10.3354/meps258019.

Bouman, H. A., C. Lepère, D. J. Scanlan, and U. Osvaldo (2012), Phytoplankton community structure in a high-nutrient, low-chlorophyll region of the eastern Pacific Subantarctic region during winter-mixed and summer-stratified conditions, *Deep Sea Res., Part I*, *69*, 1–11, doi:10.1016/j.dsr.2012.04.008.

Bricaud, A., A. Morel, M. Babin, K. Allali, and H. Claustre (1998), Variations of light absorption by suspended particles with chlorophyll a concentration in oceanic (case 1) waters: Analysis and implications for bio-optical models, *J. Geophys. Res.*, *103*(C13), 31,033–31,044, doi:10.1029/98JC02712.

Browning, T. J., H. A. Bouman, C. M. Moore, C. Schlosser, G. A. Tarran, E. M. S. Woodward, and G. M. Henderson (2014), Nutrient regimes control phytoplankton ecophysiology in the South Atlantic, *Biogeosciences*, *11*, 463–479, doi:10.5194/bg-11-463-2014.

Cassar, N., M. L. Bender, B. A. Barnett, S. Fan, W. J. Moxim, H. Levy II, and B. Tilbrook (2007), The Southern Ocean biological response to Aeolian iron deposition, *Science*, *317*(5841), 1067–1070, doi:10.1126/science.1144602.

Chekalyuk, A. M., and M. A. Hafez (2008), Advanced laser fluorometry of natural aquatic environments, *Limnol. Oceanogr. Meth.*, *6*, 591.

Cleveland, J. S., and A. D. Weidemann (1993), Quantifying absorption by aquatic particles—A multiple scattering correction for glass-fiber filters, *Limnol. Oceanogr.*, *38*(6), 1321–1327, doi:10.4319/lo.1993.38.6.1321.

Cullen, J. J. (2009), Interactive comment on "Satellite-detected fluorescence reveals global physiology of ocean phytoplankton" by M. J. Behrenfeld et al., *Biogeosci. Discuss.*, *5*, S2646–S2655.

Cullen, J. J., and R. F. Davis (2003), The blank can make a big difference in oceanographic measurements, *Limnol. Oceanogr. Bull.*, *12*, 29–35.

Cushing, D. H. (1989), A difference in structure between ecosystems in strongly stratified waters and in those that are only weakly stratified, *J. Plankton Res.*, *11*, 1–13, doi:10.1093/plankt/11.1.1.

Dandonneau, Y., and J. Neveux (1997), Diel variations of in vivo fluorescence in the eastern equatorial Pacific: An unvarying pattern, *Deep Sea Res., Part II*, *44*(9-10), 1869–1880, doi:10.1016/S0967-0645(97)00020-9.

Davey, M., G. A. Tarran, M. M. Mills, C. Ridame, R. J. Geider, and J. La Roche (2008), Nutrient limitation of picophytoplankton photosynthesis and growth in the tropical North Atlantic, *Limnol. Oceanogr.*, *53*(5), 1722–1733, doi:10.4319/lo.2008.53.5.1722.

De Baar, H. J. W., J. T. M. De Jong, D. C. E. Bakker, B. M. Loscher, C. Veth, U. Bathmann, and V. Smetacek (1995), Importance of iron for phytoplankton blooms and carbon-dioxide drawdown in the Southern Ocean, *Nature*, *373*(6513), 412–415, doi:10.1038/373412a0.

De Boyer Montégut, C., G. Madec, A. S. Fischer, A. Lazar, and D. Iudicone (2004), Mixed layer depth over the global ocean: An examination of profile data and a profile-based climatology, *J. Geophys. Res.*, *109*, C12003, doi:10.1029/2004JC002378.

Demmig-Adams, B., W. W. Adams, U. Heber, S. Neimanis, K. Winter, A. Kruger, F.-C. Czygan, W. Bilger, and O. Bjorkman (1990), Inhibition of zeaxanthin formation and of rapid changes in radiationless energy-dissipation by dithiothreitol in spinach leaves and chloroplasts, *Plant Physiol.*, *92*(2), 293–301, doi:10.1104/pp.92.2.293.

Falkowski, P. G., and D. A. Kiefer (1985), Chlorophyll-a fluorescence in phytoplankton: Relationship to photosynthesis and biomass, *J. Plankton Res.*, *7*(5), 715–731, doi:10.1093/plankt/7.5.715.

Falkowski, P. G., K. Wyman, A. C. Ley, and D. C. Mauzerall (1986), Relationship of steady-state photosynthesis to fluorescence in eucaryotic algae, *Biochim. Biophys. Acta, Bioenerg.*, *849*(2), 183–192.

Geider, R. J., J. La Roche, R. M. Greene, and M. Olaizola (1993a), Response of the photosynthetic apparatus of phaeodactylum-tricornutum (bacillariophyceae) to nitrate, phosphate, or iron starvation, *J. Phycol.*, *29*(6), 755–766, doi:10.1111/j.0022-3646.1993.00755.x.

Geider, R. J., R. M. Greene, Z. Kolber, H. L. Macintyre, and P. G. Falkowski (1993b), Fluorescence assessment of the maximum quantum efficiency of photosynthesis in the western North Atlantic, *Deep Sea Res., Part I*, *40*(6), 1205–1224, doi:10.1016/0967-0637(93)90134-O.

Gibb, S. W., R. G. Barlow, D. G. Cummings, N. W. Rees, C. C. Trees, P. Holligan, and D. Suggett (2000), Surface phytoplankton pigment distributions in the Atlantic Ocean: An assessment of basin scale variability between 50 degrees N and 50 degrees S, *Prog. Oceanogr.*, *45*(3-4), 339–368.

Holm-Hansen, O., C. J. Lorenzen, R. W. Holmes, and J. D. H. Strickland (1965), Fluorometric determination of chlorophyll, *J. Cons. Perm. Int. Explor. Mer.*, *30*, 3–15, doi:10.1093/icesjms/30.1.3.

Holm-Hansen, O., et al. (2004), Factors influencing the distribution, biomass, and productivity of phytoplankton in the Scotia Sea and adjoining waters, *Deep Sea Res., Part II*, *51*(12-13), 1333–1350, doi:10.1016/j.dsr2.2004.06.015.

Horton, P., A. V. Ruban, and R. G. Walters (1996), Regulation of light harvesting in green plants, *Annu. Rev. Plant Phys.*, *47*, 655–684.

Hu, C., F. E. Muller-Karger, C. J. Taylor, K. L. Carder, C. Kelble, E. Johns, and C. A. Heil (2005), Red tide detection and tracing using MODIS fluorescence data: A regional example in SW Florida coastal waters, *Remote Sens. Environ.*, *97*(3), 311–321, doi:10.1016/j.rse.2005.05.013.

Huot, Y., C. A. Brown, and J. J. Cullen (2005), New algorithms for MODIS sun-induced chlorophyll fluorescence and a comparison with present data products, *Limnol. Oceanogr. Meth.*, *3*, 108–130, doi:10.4319/lom.2005.3.108.

Huot, Y., B. A. Franz, and M. Fradette (2013), Estimating variability in the quantum yield of Sun-induced chlorophyll fluorescence: A global analysis of oceanic waters, *Remote Sens. Environ.*, *132*, 238–253, doi:10.1016/j.rse.2013.01.003.

©2014. American Geophysical Union. All Rights Reserved.

Kiefer, D. A., and R. A. Reynolds (1992), Advances in understanding phytoplankton fluorescence and photosynthesis, in *Primary Productivity and Biogeochemical Cycles in the Sea*, edited by P. G. Falkowski and A. D. Woodhead, pp. 155−174, Plenum, New York.
Kiefer, D. A., W. S. Chamberlin, and C. R. Booth (1989), Natural fluorescence of chlorophyll-a: Relationship to photosynthesis and chlorophyll concentration in the western South-Pacific gyre, *Limnol. Oceanogr.*, *34*(5), 868–881.
Kishino, M., M. Takahashi, N. Okami, and S. Ichimura (1985), Estimation of the spectral absorption coefficients of phytoplankton in the sea, *Bull. Mar. Sci.*, *37*(2), 634–642.
Kolber, Z., J. Zehr, and P. Falkowski (1988), Effects of growth irradiance and nitrogen limitation on photosynthetic energy conversion in photosystem II, *Plant Physiol.*, *88*(3), 923–929, doi:10.1104/pp.88.3.923.
Kolber, Z. S., O. Prasil, and P. G. Falkowski (1998), Measurements of variable chlorophyll fluorescence using fast repetition rate techniques: Defining methodology and experimental protocols, *Biochim. Biophys. Acta, Bioenerg.*, *1367*(1-3), 88–106, doi:10.1016/S0005-2728(98)00135-2.
Korb, R. E., M. J. Whitehouse, A. Atkinson, and S. E. Thorpe (2008), Magnitude and maintenance of the phytoplankton bloom at South Georgia: A naturally iron-replete environment, *Mar. Ecol. Prog. Ser.*, *368*, 75–91, doi:10.3354/meps07525.
Lavaud, J., R. F. Strzepeck, and P. G. Kroth (2007), Photoprotection capacity differs among diatoms: Possible consequences on the spatial distribution of diatoms related to fluctuations in the underwater light climate, *Limnol. Oceanogr.*, *52*, 1188–1194, doi:10.4319/lo.2007.52.3.1188.
Lee, Z. P., K. L. Carder, and R. A. Arnone (2002), Deriving inherent optical properties from water color: A multiband quasi-analytical algorithm for optically deep waters, *Appl. Opt.*, *41*(27), 5755–5772, doi:10.1364/AO.41.005755.
Lefèvre, N., and A. J. Watson (1999), Modeling the geochemical cycle of iron in the oceans and its impact on atmospheric CO_2 concentrations, *Global Biogeochem. Cycles*, *13*(3), 727–736, doi:10.1029/1999GB900034.
Letelier, R. M., M. R. Abbott, and D. M. Karl (1997), Chlorophyll natural fluorescence response to upwelling events in the Southern Ocean, *Geophys. Res. Lett.*, *24*(4), 409–412, doi:10.1029/97GL00205.
Longhurst, A. R. (1998), *Ecological Geography of the Sea*, Academic Press, San Diego, Calif.
Mackey, M. D., D. J. Mackey, H. W. Higgins, and S. W. Wright (1996), CHEMTAX—A program for estimating class abundances from chemical markers: Application to HPLC measurements of phytoplankton, *Mar. Ecol. Prog. Ser.*, *144*(1-3), 265–283, doi:10.3354/meps144265.
Margalef, R. (1978), Life-forms of phytoplankton as survival alternatives in an unstable environment, *Oceanol. Acta*, *1*, 493–509.
Maritorena, S., A. Morel, and B. Gentili (2000), Determination of the fluorescence quantum yield by oceanic phytoplankton in their natural habitat, *Appl. Opt.*, *39*(36), 6725–6737, doi:10.1364/AO.39.006725.
Milligan, A. J., U. A. Aparicio, and M. J. Behrenfeld (2012), Fluorescence and nonphotochemical quenching responses to simulated vertical mixing in the marine diatom *Thalassiosira weissflogii*, *Mar. Ecol. Prog. Ser.*, *448*, 67–78, doi:10.3354/meps09544.
Milne, A., W. Landing, M. Bizimis, and P. Morton (2010), Determination of Mn, Fe, Co, Ni, Cu, Zn, Cd and Pb in seawater using high resolution magnetic sector inductively coupled mass spectrometry (HR-ICP-MS), *Anal. Chim. Acta*, *665*(2), 200–207, doi:10.1016/j.aca.2010.03.027.
Mitchell, B. G., and O. Holm-Hansen (1991), Bio-optical properties of Antarctic Peninsula waters—Differentiation from temperate ocean models, *Deep Sea Res. Part A*, *38*(8–9), 1009–1028, doi:10.1016/0198-0149(91)90094-V.
Moore, C. M., S. Seeyave, A. E. Hickman, J. T. Allen, M. I. Lucas, H. Planquette, R. T. Pollard, and A. J. Poulton (2007), Iron-light interactions during the CROZet natural iron bloom and EXport experiment (CROZEX) I: Phytoplankton growth and photophysiology, *Deep Sea Res., Part II*, *54*, 2045–2065, doi:10.1016/j.dsr2.2007.06.011.
Moore, C. M., M. M. Mills, R. Langlois, A. Milne, E. P. Achterberg, J. La Roche, and R. J. Geider (2008), Relative influence of nitrogen and phosphorus availability on phytoplankton physiology and productivity in the oligotrophic sub-tropical North Atlantic Ocean, *Limnol. Oceanogr.*, *53*(1), 291–305, doi:10.4319/lo.2008.53.1.0291.
Moore, C. M., et al. (2013), Processes and patterns of oceanic nutrient limitation, *Nat. Geosci.*, *6*, 701–710, doi:10.1038/ngeo1765.
Morel, A., and A. Bricaud (1981), Theoretical results concerning light-absorption in a discrete medium, and application to specific absorption of phytoplankton, *Deep Sea Res. Part A*, *28*(11), 1375–1393, doi:10.1016/0198-0149(81)90039-X.
Morrison, J. R. (2003), In situ determination of the quantum yield of phytoplankton chlorophyll a fluorescence: A simple algorithm, observations, and a model, *Limnol. Oceanogr.*, *48*(2), 618–631, doi:10.4319/lo.2003.48.2.0618.
Morrison, J. R., and D. S. Goodwin (2010), Phytoplankton photocompensation from space-based fluorescence measurements, *Geophys. Res. Lett.*, *37*, L06603, doi:10.1029/2009GL041799.
Müller, P., X. P. Li, and K. K. Niyogi (2001), Non-photochemical quenching. A response to excess light energy, *Plant Physiol.*, *125*(4), 1558–1566, doi:10.1104/pp.125.4.1558.
Naveira Garabato, A. C., K. L. Polzin, B. A. King, K. J. Heywood, and M. Visbeck (2004), Widespread intense turbulent mixing in the Southern Ocean, *Science*, *303*(5655), 210–213, doi:10.1126/science.1090929.
Orsi, A. H., T. Whitworth III, and W. D. Nowlin, Jr. (1995), On the meridional extent and fronts of the Antarctic Circumpolar Current, *Deep Sea Res., Part I*, *42*, 641–673, doi:10.1016/0967-0637(95)00021-W.
Parkhill, J. P., G. Maillet, and J. J. Cullen (2001), Fluorescence-based maximal quantum yield for PSII as a diagnostic of nutrient stress, *J. Phycol.*, *37*(4), 517–529, doi:10.1046/j.1529-8817.2001.037004517.
Raiswell, R., L. G. Benning, M. Tranter, and S. Tulaczyk (2008), Bioavailable iron in the Southern Ocean: The significance of the iceberg conveyor belt, *Geochem. Trans.*, *9*, 7, doi:10.1186/1467-4866-9-7.
Raven, J. A. (2011), The cost of photoinhibition, *Physiol. Plant.*, *142*(1), 87–104, doi:10.1111/j.1399-3054.2011.01465.x.
Reynolds, R. A., D. Stramski, and B. G. Mitchell (2001), A chlorophyll-dependent semianalytical reflectance model derived from field measurements of absorption and backscattering coefficients within the Southern Ocean, *J. Geophys. Res.*, *106*(C4), 7125–7138, doi:10.1029/1999JC000311.
Ryan-Keogh, T. J., A. I. Macey, A. M. Cockshutt, C. M. Moore, and T. S. Bibby (2012), The cyanobacterial chlorophyll-binding-protein IsiA acts to increase the in vivo effective absorption cross-section of psi under iron limitation, *J. Phycol.*, *48*(1), 145–154, doi:10.1111/j.1529-8817.2011.01092.x.
Ryan-Keogh, T. J., A. I. Macey, M. C. Nielsdóttir, M. I. Lucas, S. S. Steigenberger, M. C. Stinchcombe, E. P. Achterberg, T. S. Bibby, and C. M. Moore (2013), Spatial and temporal development of phytoplankton iron stress in relation to bloom dynamics in the high-latitude North Atlantic Ocean, *Limnol. Oceanogr.*, *58*(2), 533–545, doi:10.4319/lo.2013.58.2.0533.
Sakshaug, E., and O. Holm-Hansen (1977), Chemical composition of skeletonema-costatum (grev) cleve and pavlova (monochrysis) lutheri (droop) green as a function of nitrate-limited, phosphate-limited, and iron-limited growth, *J. Exp. Mar. Biol. Ecol.*, *29*(1), 1–34.
Sathyendranath, S., G. Cota, V. Stuart, H. Maass, and T. Platt (2001), Remote sensing of phytoplankton pigments: A comparison of empirical and theoretical approaches, *Int. J. Remote Sens.*, *22*(2-3), 249–273, doi:10.1080/014311601449925.
Schallenberg, C., M. R. Lewis, D. E. Kelley, and J. J. Cullen (2008), Inferred influence of nutrient availability on the relationship between Sun-induced chlorophyll fluorescence and incident irradiance in the Bering Sea, *J. Geophys. Res.*, *113*, C07046, doi:10.1029/2007JC004355.

©2014. American Geophysical Union. All Rights Reserved.

Schrader, P. S., A. J. Milligan, and M. J. Behrenfeld (2011), Surplus photosynthetic antennae complexes underlie diagnostics of iron limitation in a cyanobacterium, *PLoS One*, *6*(4), e18753, doi:10.1371/journal.pone.0018753.

Strzepek, R. F., and P. J. Harrison (2004), Photosynthetic architecture differs in coastal and oceanic diatoms, *Nature*, *431*(7009), 689–692, doi:10.1038/nature02954.

Stuart, V., S. Sathyendranath, E. J. H. Head, T. Platt, B. Irwin, and H. Maass (2000), Bio-optical characteristics of diatom and prymnesiophyte populations in the Labrador Sea, *Mar. Ecol. Prog. Ser.*, *201*, 91–106, doi:10.3354/meps201091.

Suggett, D. J., C. M. Moore, A. E. Hickman, and R. J. Geider (2009), Interpretation of fast repetition rate (FRR) fluorescence: Signatures of phytoplankton community structure versus physiological state, *Mar. Ecol. Prog. Ser.*, *376*, 1–19, doi:10.3354/meps07830.

Topliss, B. J., and T. Platt (1986), Passive fluorescence and photosynthesis in the ocean—Implications for remote-sensing, *Deep Sea Res. Part A*, *33*(7), 849–864.

Veldhuis, M. J. W., and G. W. Kraay (2004), Phytoplankton in the subtropical Atlantic Ocean: Towards a better assessment of biomass and composition, *Deep Sea Res., Part I*, *51*(4), 507–530, doi:10.1016/j.dsr.2003.12.002.

Venables, H., and C. M. Moore (2010), Phytoplankton and light limitation in the Southern Ocean: Learning from high-nutrient, high-chlorophyll areas, *J. Geophys. Res.*, *115*, C02015, doi:10.1029/2009JC005361.

Westberry, T. K., M. J. Behrenfeld, A. J. Milligan, and S. C. Doney (2013), Retrospective satellite ocean color analysis of purposeful and natural ocean iron fertilization, *Deep Sea Res., Part I*, *73*, 1–16, doi:10.1016/j.dsr.2012.11.010.

Woodward, E. M. S., and A. P. Rees (2001), Nutrient distributions in an anticyclonic eddy in the North East Atlantic Ocean, with reference to nanomolar ammonium concentrations, *Deep Sea Res., Part II*, *48*, 775–794.

Wright, S. W., D. P. Thomas, H. J. Marchant, H. W. Higgins, M. D. Mackey, and D. J. Mackey (1996), Analysis of phytoplankton of the Australian sector of the Southern Ocean: Comparisons of microscopy and size frequency data with interpretations of pigment HPLC data using the 'CHEMTAX' matrix factorisation program, *Mar. Ecol. Prog. Ser.*, *144*(1–3), 285–298, doi:10.3354/meps144285.

©2014. American Geophysical Union. All Rights Reserved.